*29th EPS Conference on Plasma Phys. and Contr. Fusion Montreux, 17-21 June 2002 ECA Vol. **26B**, P-5.082 (2002)*

Role of Radial Electric Field Control in the Tandem Mirror Plasma

K.Ishii, Y.Takemura, A.Fueki, M.Shimoo, K.Tsutsui, K.Hagisawa, A.Kojima, I.Katanuma,

T.Saito, A.Itakura, K.Yatsu

Plasma Research Center, University of Tsukuba, Ibaraki 305-8577, Japan

After improvement of axial confinement by creation of confining potentials, the radial confinement came up as an important subject in the tandem mirror. We paid attention to the radial drift of ions passing through the anchor cells with nonaxisymmetric magnetic configuration. Radial drift of the passing ions was estimated as a function of a defined deformation factor. Radial potential profile of the core plasma was experimentally controlled by changing the end plate potentials. Flattened radial potential profile was effective for the decrease of radial transport as shown in the calculated results.

1. Introduction

In the tandem mirror, electrostatic potentials are created on both sides of the plasma in order to improve the axial confinement.[1] Microwaves are injected into the plug region to produce the confining potential. Existence of the plug potential bounce ion reflected by the plug potential is essential to increase the plasma density in the central cell. The plug potential bounce ion and outer mirror throat bounce ion were observed directly in decay phase of the plug potential using an end-loss energy component analyzer (ELECA).[2] On the other hand, anchor cells with nonaxisymmetric magnetic configuration are included between the central solenoid and the plug/barrier cells. High potential formed by electron heating causes strong radial electric field at the anchor mirror region with the strongly deformed magnetic flux tube. If the shape of the cross section of the magnetic flux tube is shifted from the cross section of the equipotential surface, trajectories of the ion passing through the anchor cell are seemed to be affected and shifted radially. We calculated the ion trajectories and estimated the influence of the radial drift of ions on the discrepancy of the cross section shapes as a function of a defined deformation factor (Df). It was found that the increase of the discrepancy enhanced the radial drift of the passing ions. Experimentally the radial potential profiles of the core plasma were adjusted by controlling the electrostatic potentials of the coaxially separated end plates located on both ends of the machine. We observed that the flattened radial potential profile of the core plasma was effective for the decrease of the radial transport of ion.

2. Bounce Area in Epsilon-Mu Space

The tandem mirror GAMMA 10 is consist of the central solenoid, nonaxisymmetric

anchor cells with the minimum-B magnetic field configuration and axisymmetric plug/barrier cells as shown in Fig.1.[3] The magnetic field strength in the mirror throats of the central cell and the anchor cell is almost the same (~20 kG). The mirror throat of the plug/barrier cell is the strongest (~30 kG) in the magnetic system. Initial plasmas are injected into the machine from both ends of the tandem mirror along the magnetic field line, and then main plasma is produced, maintained and heated by ion cyclotron range of frequency (ICRF) waves. Microwaves are also injected into the plug and barrier regions in the plug/barrier cell and electron cyclotron resonance heating (ECRH) is carried out to create confining potential and thermal barrier potential.

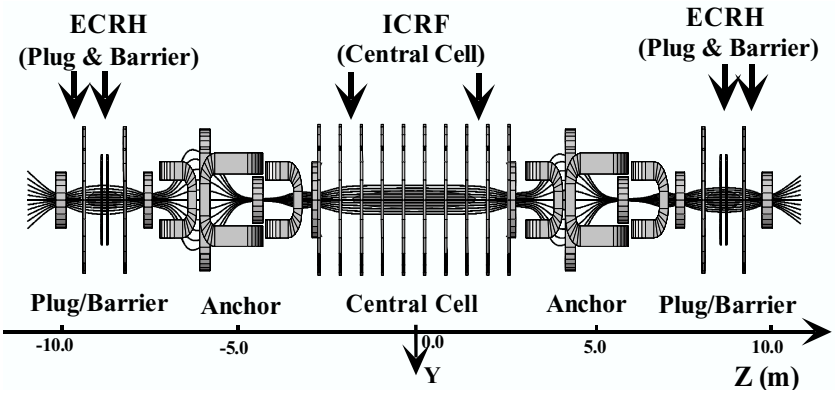

Fig.1
Locations of magnetic coils and heating systems.

In open systems there exists necessarily loss regions in the velocity space of the plasma. Ions scattered from the trapped region to the loss region are decreased by shifting the loss boundaries to the higher energy side due to creation of the confining potential, and the axial confinement is improved. Ions are roughly classified into the end-loss ion, the outer mirror throat (OMT) bounce ion, the plug potential (PP) bounce ion, inner mirror throat (IMT) bounce ion, the plug/barrier (PB) trapped ion, anchor mirror (AM) trapped ion and the central mirror (CM) trapped ion as shown in Fig.2. The PP bounce ion is bounced near the plug potential region. If relatively high potential is produced between the plug region and the outer mirror throat, some ions with high energy passed through the plug potential are bounced near the outer mirror throat as the OMT bounce ion. Each region is separated in the ε-μ space in Fig.3, where ε and μ are the energy and the magnetic moment, respectively.

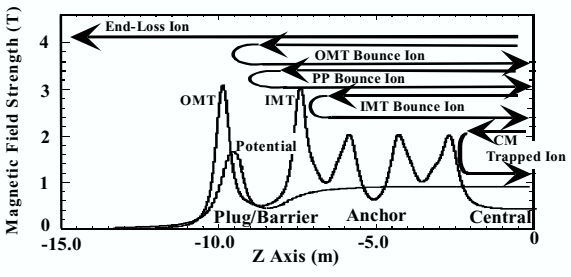

Fig.2
Schematic diagram of bounce ions and trapped ions.

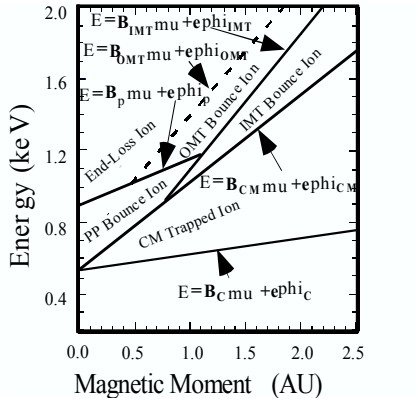

Fig.3
Bounce area in the ε-μ space.

3. Observation of OMT Bounce Ion

Loss boundaries of the PP bounce region and the IMT bounce region are described as two lines of $\varepsilon = B_P\mu + e\phi_P$ and $\varepsilon = B_{IMT}\mu + e\phi_{IMT}$ in the ε-μ space, respectively. As the magnetic field strength of the IMT and OMT regions is almost the same and the strongest, the OMT bounce ion exists in case that potential near the OMT region is higher than the IMT potential, and also the OMT bounce region extends up to higher energy area than the PP bounce region. When the IMT potential becomes low with formation of the thermal barrier potential as compared with the plasma without potential plugging, outflow of the IMT bounce ion is not observed on turning off the microwave injection for the ECRH. On the other hand the OMT bounce ion may be observed in the decay phase of the plug potential formation. From the above point of view, we paid attention to measurement of time evolution of the end-loss ion using an end-loss energy component analyzer (ELECA).

Figure 4 shows time evolution of line density in the central cell and electrostatic potentials in the central, barrier and plug cells. When the microwave injection was turned on, the plug potential was created and the barrier potential was decreased, then the central line density increased. As the plug potential is about 700V, the upper energy of the PP bounce region is about 1 kV at most. We measured time evolution of the end-loss current by applying the chopping wave form voltage on the electrodes of the analyzer, and observed the peaking loss current due to the end-loss ion with higher energy than the upper energy of the PP bounce region. Figure 5 shows as an example the end-loss current density with the ion energy between 1.85 keV and 2.15 keV. The peaking loss current due to the OMT bounce ion appeared clearly in decay phase of the confining potential.

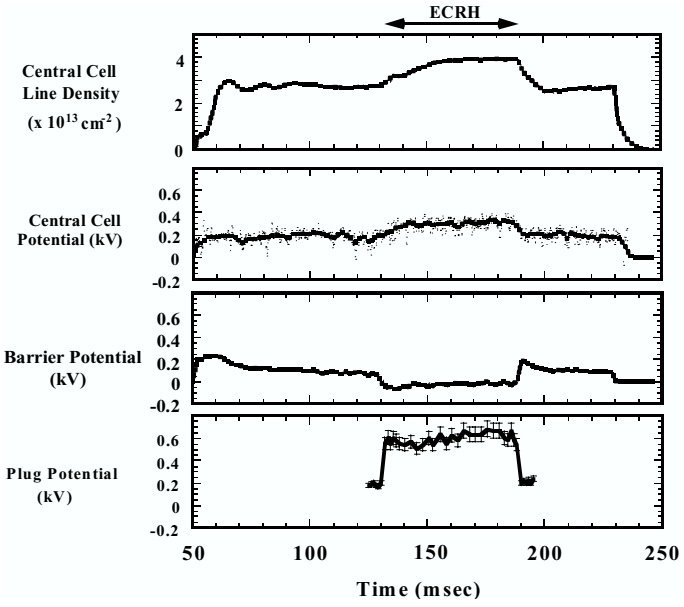

Fig.4 Time evolution of density and potentials.

Two types of decay time were also observed, that is, one was caused by transit time (several 10 μsec) of the PP bounce ion and the OMT bounce ion and the other was caused by collision time (several msec) flowing into the loss region from the trapped region. We confirmed outflow of the PP bounce ion and the OMT bounce ion.

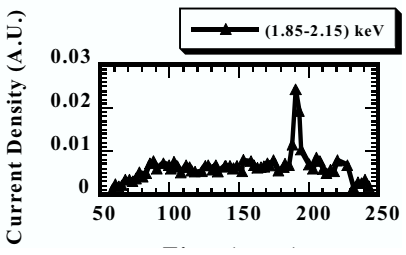

Fig.5 Peaking loss current density.

4. Calculation of Ion Trajectories and Experimental Results

We defined the deformation factor D_f as follows, $r_h(z) = r_{hf}(z) - (r_{hf}(z) - r_h(0))D_f$, here $2r_h(z)$ is the full width at half maximum of the radial potential profile at z, and $r_{hf}(z)$ is the radius of the magnetic flux tube at z, here $r_{hf}(0) = r_h(0)$. We assumed that the peak potential (at x = y = z =0) was 300 V and $r_h(0)$=0.07 m. Ions were initially situated at equal interval (20 degrees) on a circumference of a circle with the radius 0.05 m located on the mid-plane of the central cell. We calculated the trajectories of ions with the energy of 0.5 and 1 keV and estimated the ions radially drifted outside the circle with the radius 0.1 m after a half bounce as shown in Fig.6. The radial drift was enhanced by discrepancy of shapes between the magnetic flux tube and the equipotential surface.

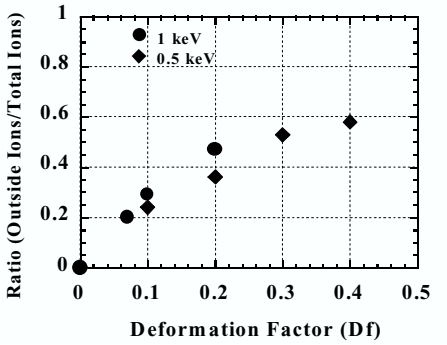

Fig.6 Dependence of radial drift on deformation factor.

It was observed that the electrostatic potential usually increased in the central cell by carrying out ECRH at the plug region and also the radial slope of the potential profile became steeper, by the potential measurement using a gold neutral beam probe method. We controlled the radial electric field of the core plasma by changing the electrostatic potential of the coaxially separated end plates without changing the radiation pattern of the plug microwaves. The end plates consisted of 5 portions, and each portion was connected to grounded plate through electric resistance. The endplate potential was changed by adjusting the end plate current as shown in Fig.7.

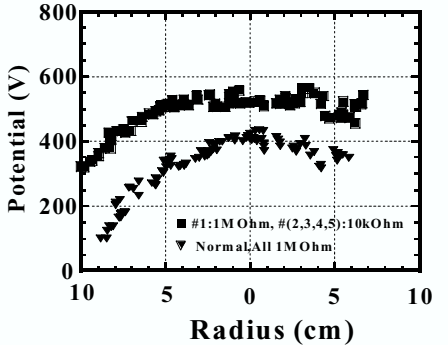

Fig.7 Radial potential profile.

The quantity of the PP and OMT bounce ions was estimated from the peaking loss current of end-loss ions. Relaxation of the radial transport due to the flatted radial potential profile of the core plasma was found by analyzing the plasma density in the central cell and the peaking outflow of the PP and OMT bounce ions appeared just after turning off the ECRH. Figure 8 is the relation of the end-loss current ratio to the radial electric field.

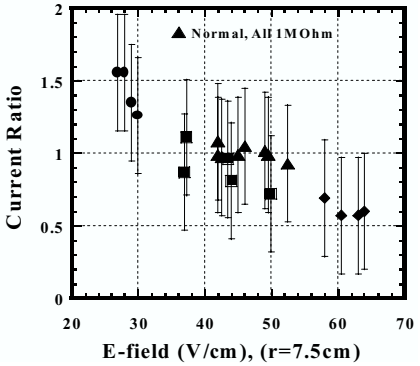

Fig.8 Ratio is normalized normal resistance current.

Reference

[1] G.I.Diimov et al., Sov. J. Plasma Phys. Vol.2, (1976)326.
[2] K.Ishii, et al., J. Phys. Soc. Jpn. Vol.66, (1997) 2224.
[3] M.Inutake, et al., Fusion Reactor Design and Technology (IAEA, Vienna, 1983) Vol.1, p.429.